10-1-2008

Electrical actuation of electrically conducting and insulating droplets using ac and dc voltages

Niru Kumari
Purdue University, nkumari@purdue.edu

Vaibhav Bahadur
Purdue University - Main Campus, vbahadur@purdue.edu

Suresh Garimella
School of Mechanical Engineering, Birck Nanotechnology Center, Purdue University, sureshg@purdue.edu

J. Micromech. Microeng. **18** (2008) 105015 (10pp) doi:10.1088/0960-1317/18/10/105015

Electrical actuation of electrically conducting and insulating droplets using ac and dc voltages

N Kumari, V Bahadur and S V Garimella

School of Mechanical Engineering and Birck Nanotechnology Center, Purdue University, West Lafayette, IN 47907-2088, USA

E-mail: sureshg@purdue.edu

Received 18 June 2008, in final form 15 August 2008
Published 10 September 2008
Online at stacks.iop.org/JMM/18/105015

Abstract

Electrical actuation of liquid droplets at the microscale offers promising applications in the fields of microfluidics and lab-on-chip devices. Much prior research has targeted the electrical actuation of electrically conducting liquid droplets using dc voltages (classical electrowetting). Electrical actuation of conducting droplets using ac voltages and the actuation of insulating droplets (using dc or ac voltages) has remained relatively unexplored. This paper utilizes an energy-minimization-based analytical framework to study the electrical actuation of a liquid droplet (electrically conducting or insulating) under ac actuation. It is shown that the electromechanical regimes of classical electrowetting, electrowetting under ac actuation and insulating droplet actuation can be extracted from the generic electromechanical actuation framework, depending on the electrical properties of the droplet, the underlying dielectric layer and the frequency of the actuation voltage. This paper also presents experiments which quantify the influence of the ac frequency and the electrical properties of the droplet on its velocity under electrical actuation. The velocities of droplets moving between two parallel plates under ac actuation are experimentally measured; these velocities are then related to the actuation force on the droplet which is predicted by the electromechanical model developed in this work. It is seen that the droplet velocities are strongly dependent on the frequency of the ac actuation voltage; the cut-off ac frequency, above which the droplet fails to actuate, is experimentally determined and related to the electrical conductivity of the liquid. This paper then analyzes and directly compares the various electromechanical regimes for the actuation of droplets in microfluidic applications.

(Some figures in this article are in colour only in the electronic version)

1. Introduction

Electrical actuation and control of fluid motion at the microscale has significant applications in the areas of microfluidics and lab-on-chip devices. Electrical actuation of electrically conducting droplets has received significant research attention over the past decade. Electrowetting (EW) [1], for example, has been extensively studied [2–7] as a tool to actuate and control electrically conducting droplets. The classical analyses of the EW systems are based on the premise of the droplet being a perfect electrical conductor. Water droplets are made electrically conducting by adding a small amount of salt (e.g., potassium chloride). However, experimentation has shown that even low electrical conductivity liquids and even perfectly insulating liquids can be actuated by electrical means. Chatterjee *et al* [5] actuated 29 different liquids comprising organic solvents, ionic liquids and surfactant solutions in the same setup as that used for actuating electrically conducting droplets. Many of the liquids actuated by Chatterjee *et al* [5] had very low electrical conductivities and cannot be considered perfectly conducting.

Microelectronics applications which involve direct contact of the liquid with an electronic component necessarily require the use of electrically insulating liquids. Insulating

liquids are also typically much less corrosive than the electrically conducting alternatives. Very little published work is available on the electrical actuation of perfectly insulating fluid elements despite the advantages resulting from the use of insulating liquids. Pellat [8] performed a classical experiment in 1895 which consisted of drawing up a finger of transformer oil between two parallel plates through the application of an electrical voltage. Jones *et al* [9] demonstrated a voltage-induced height rise of a transformer oil finger (between two parallel plates with a separation of 1 mm). Kumari *et al* [10] recently demonstrated the electrical actuation of insulating fluids by experimentally measuring the velocities of transformer oil droplets moving between two flat plates under a dc voltage.

Another notable feature of the available research on EW involves the use of dc electrical voltages to move electrically conducting droplets. While it has been demonstrated [5, 11–13] that ac voltages can also actuate droplets, there is little available research on the influence of ac voltages on the actuation of liquid droplets. Use of ac voltages for electrical actuation is advantageous since the possibility of chemical reactions in the droplet is minimized [5]. Additionally, Berge and Peseux [14] have reported a reduction in contact-angle hysteresis upon the use of ac voltages; this should reduce the threshold voltage for ac actuation. The most extensive study utilizing ac voltages was carried out by Chatterjee *et al* [5], wherein 29 liquids were tested for electrical actuation between two flat plates using an ac voltage. Successful actuation was seen to be dependent on the frequency of the ac voltage and plate spacing; reduction in the ac frequency and reduction in plate spacing were shown to be conducive to actuation. Kumar *et al* [12] studied the contact angle variation of aqueous salt solutions under a variable-frequency ac voltage. Ko *et al* [15] carried out experimental visualizations of the flow field inside a droplet oscillating under the influence of a variable-frequency ac voltage. Jones [9] used an ac voltage to actuate a finger of perfectly insulating transformer oil.

It is clear that none of the above results can be explained using the classical electrowetting theory, which relies on the assumption of a perfectly conducting droplet. There is limited available work on the development of a model which accounts for the effect of the ac frequency, the electrical properties of the droplet and the underlying dielectric layer and geometry on the electrical actuation of a generic liquid droplet. Chatterjee *et al* [5] attempted to relate droplet actuation to the frequency-dependent complex permittivity of the fluid; however many of the results of that work cannot be explained based on the fluid complex permittivity alone. Kumar *et al* [12] proposed a simplified RC circuit model to explain the contact angle variation of aqueous salt solutions. Hong *et al* [16] carried out detailed numerical modeling to predict the contact angle variation of a droplet with frequency of the ac voltage. Their numerical simulations showed that the electric field inside a droplet is very strongly dependent on the ac frequency; at a sufficiently high ac frequency, an electrically conducting droplet behaves like an insulating droplet due to the penetration of the electric field inside the droplet. A more generalized theory of electrical actuation of fluids has been developed [17–19] to understand the relationship between electrowetting and dielectrophoretic actuation. It has been demonstrated that electrowetting and dielectrophoresis are the low- and high-frequency limits of the electromechanical response of a fluid to an electrical signal.

The study of electrical actuation of a generic liquid droplet (electrically conducting or insulating) using ac voltages can build upon the extensive studies available in the field of EW-induced droplet movement. Phenomena which influence classical EW systems such as contact-line friction influence the actuation of all liquid droplets. Additionally, the flow fields inside a droplet under any kind of electrical actuation are expected to be similar. Consequently, much of the knowledge of EW-induced conducting droplet motion can be directly applied to the study of the actuation of a generic liquid droplet. Phenomena which influence classical EW systems, such as contact-angle saturation, contact-angle hysteresis and interface ion adsorption show different results when ac voltages are used instead of dc voltages; however, the present work is not intended to analyze these differences.

The primary objective of this paper is to analyze classical EW, EW using ac voltages and the actuation of insulating droplets under a common electromechanical framework. An analytical model, based on scaling arguments is developed to estimate the actuation force acting on a droplet (electrically conducting or insulating) moving between two plates under an ac voltage. The regimes of classical EW, EW using ac voltages, and the actuation of insulating droplets are extracted from this general model, depending on the electrical properties (electrical conductivity and dielectric constant) of the droplet and the underlying dielectric layer, the ac frequency and droplet geometry. Experiments are carried out to study and analyze these three different regimes of electromechanical actuation. These experiments comprise the measurement of droplet velocities with multiple fluids (having different electrical conductivities) as a function of ac frequency. The measured droplet velocities are a direct measure of the actuation force on the droplet and are used to analyze the predictions of the actuation force model. It is seen that the measured droplet velocities decrease with an increase in ac frequency; the cut-off frequency (above which droplet motion is arrested) is experimentally measured for multiple fluids. The experimentally obtained droplet velocities for the case of classical EW and EW using ac voltages are then compared with the experimentally measured velocities during the actuation of an insulating transformer oil droplet [10]; this comparison is then used to analyze various aspects of the three different regimes of electrical actuation (classical EW, EW under ac actuation and insulating droplet actuation).

2. An actuation model for a generic liquid droplet

2.1. A representative droplet actuation device

A schematic representation of a device that can bring about electrical actuation of liquid droplets is shown in figure 1, and is similar to the configuration used for EW-induced actuation of electrically conducting liquids [2]. It consists of two flat

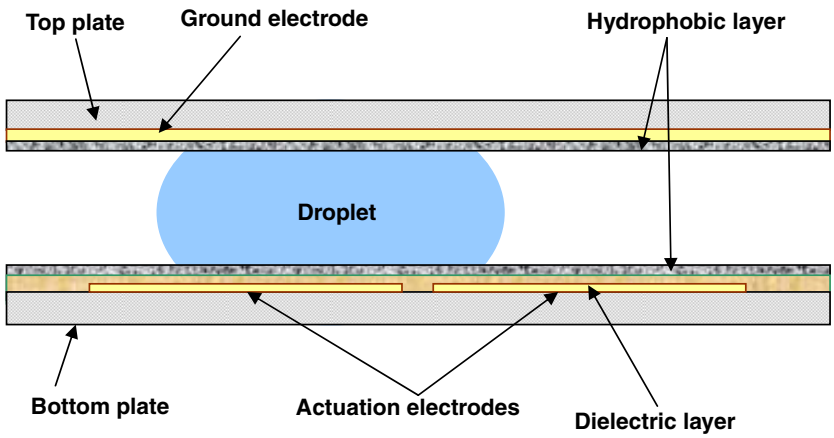

Figure 1. Representative device for electrical actuation of droplets [10].

plates separated by a known spacing. An array of electrodes on the bottom plate is used to actuate the droplet. The top plate has a continuous electrode which serves as the ground electrode and ensures complete droplet transition to the actuated electrode [2]. The electrodes on the bottom plate are covered with a dielectric layer to prevent chemical reactions between the ions in the droplet and the metal electrodes. The top plate does not have a dielectric layer so that the electrical actuation force on the droplet may be maximized [2]. A hydrophobic layer of Teflon is coated on both plates to ensure high initial contact angles.

2.2. *Analytical model for actuation force estimation*

An electromechanical framework is utilized in the present work to estimate the actuation force on a liquid droplet. For the most general case of actuation, the electric field lines penetrate the dielectric layer as well as the droplet. Additionally, the electric field distribution is dependent on the position of the droplet. In the present work, the actuation force on all droplets is estimated only at the midpoint of the transition using a simplified analytical model. All actuation force comparisons are carried out only at the midpoint of the transition; the actuation force comparison at other transition positions would be expected to be similar in nature. The droplet is sandwiched between the two plates with a separation of H as shown in figure 2(a). The top plate and the left electrode on the bottom plate are grounded and the right electrode serves as the actuation electrode. The dielectric thickness covering the bottom electrodes is h. The coordinate system to track the leading edge of the droplet is located at the center of the intersection line of the two electrodes on the bottom plate as shown in figure 2(b). The droplet is assumed to maintain its circular shape (in plan view) during the transition, and any deformation induced during its movement by contact-line friction is neglected.

The electromechanical response of any material to an applied electric field can be studied by modeling the material as a resistor in parallel with a capacitor. The resistance represents the electrical conductivity of the material, whereas the capacitance represents the dielectric behavior of the

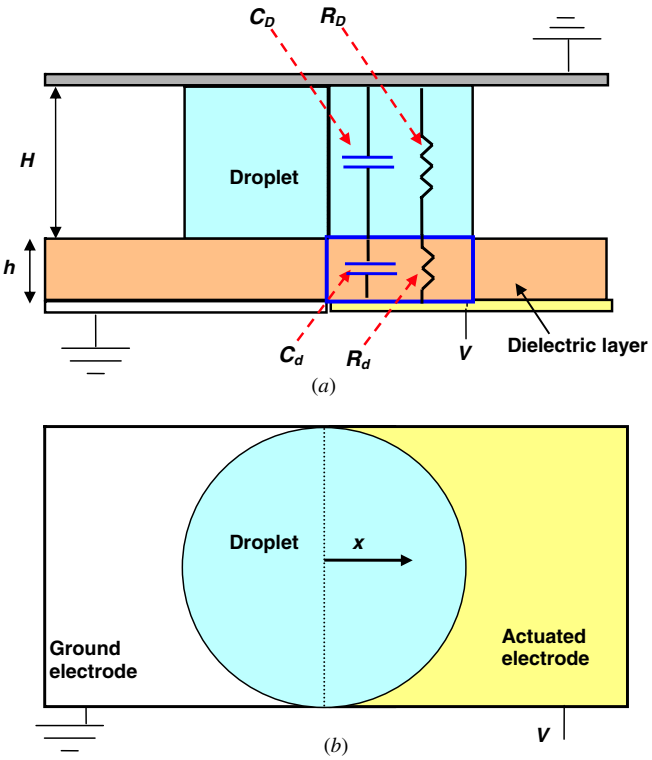

Figure 2. Schematic illustration of a droplet at the midpoint of the transition: (a) side view and (b) top view.

material. The energy stored in the capacitive part of the material provides the motive force for droplet actuation, while the energy dissipated in the resistive part of the material leads to Joule heating. The capacitive and resistive components of any material can be combined into one useful parameter, the complex permittivity [5], which is defined as

$$\varepsilon^* = k\varepsilon_0 - \mathrm{j}\frac{\sigma}{\omega}, \tag{1}$$

where k is the dielectric constant, σ the electrical conductivity, ε_0 the permittivity of vacuum and ω is the frequency of the applied ac voltage. The first and the second terms in equation (1) denote the capacitive and resistive components of the complex permittivity, respectively. It is seen that

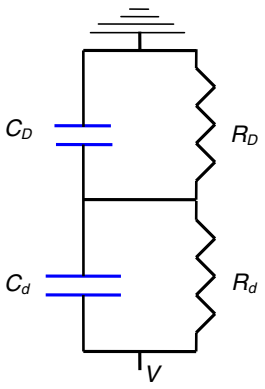

Figure 3. The RC network used to estimate the actuation force on a generic liquid droplet.

the contribution of the electrical conductivity to the complex permittivity decreases with the frequency of the ac signal. This implies that an electrically conducting droplet will behave like a dielectric droplet at sufficiently high ac frequencies [16]. The complex capacitance can be defined using the complex permittivity as

$$C^* = \frac{A\varepsilon^*}{l} = C - \frac{\mathrm{j}}{R\omega}, \tag{2}$$

where C is the capacitance, R is the electrical resistance, A is the cross-section area and l is the length of the material.

Within this framework, the simplest model for studying the actuation of a generic liquid droplet includes the resistance and capacitance of the droplet and that of the underlying dielectric layer. Figure 3 shows a simplified RC model for estimating the actuation force on a generic droplet undergoing motion between two parallel plates as described in figure 2. This first-order model is based on a scaling analysis and estimates the actuation force at the midpoint of the transition. This model accounts for the electric field lines which originate from the right bottom electrode (figure 2(*a*)) and terminate on the top electrode. This implies that the contribution of the droplet and the dielectric on the left electrode is not accounted for in the present model. A more detailed model could capture the contribution of the part of the droplet and dielectric on the left electrode; however, the present work is targeted at understanding various electromechanical actuation regimes and the scaling-based model presented below serves this purpose. With these assumptions, the RC network consists of the dielectric layer and droplet capacitances C_d and C_D, respectively, and the dielectric layer and droplet resistances R_d and R_D, respectively.

The capacitances and resistances in the above circuit can be estimated as

$$C_d = \frac{Ak_d\varepsilon_0}{h} \quad \text{and} \quad C_D = \frac{Ak_D\varepsilon_0}{H} \tag{3}$$

and

$$R_d = \frac{h}{\sigma_d A} \quad \text{and} \quad R_D = \frac{H}{\sigma_D A}, \tag{4}$$

where (k_d, σ_d) and (k_D, σ_D) are the (dielectric constant, electrical conductivity) of the dielectric layer and the droplet, respectively, and A is the area of the droplet on the actuated electrode. The total impedances Z_d and Z_D of the dielectric layer and the droplet can be expressed in terms of the frequency ω of the ac voltage as

$$Z_d = \frac{R_d}{1 + \mathrm{j}(\omega R_d C_d)} \quad \text{and} \quad Z_D = \frac{R_D}{1 + \mathrm{j}(\omega R_D C_D)}, \tag{5}$$

where $\omega = 2\pi f$ is the angular frequency corresponding to the frequency f of the ac voltage.

The total impedance of the droplet and the dielectric layer can be expressed as

$$Z_{\mathrm{eq}} = Z_d + Z_D = \left(\frac{R_d}{1 + (\omega R_d C_d)^2} + \frac{R_D}{1 + (\omega R_D C_D)^2}\right) - \mathrm{j}\omega\left(\frac{R_d^2 C_d}{1 + (\omega R_d C_d)^2} + \frac{R_D^2 C_D}{1 + (\omega R_D C_D)^2}\right). \tag{6}$$

The total impedance of the circuit can be used to estimate the effective complex capacitance of the circuit as

$$C^*_{\mathrm{eq}} = \frac{1}{\mathrm{j}\omega Z_{\mathrm{eq}}}. \tag{7}$$

The above expression is used to estimate the effective capacitance of the system as

$$C_{\mathrm{eq}} = \frac{\left(\frac{R_d^2 C_d}{1+(\omega R_d C_d)^2} + \frac{R_D^2 C_D}{1+(\omega R_D C_D)^2}\right)}{\left(\left(\frac{R_d}{1+(\omega R_d C_d)^2} + \frac{R_D}{1+(\omega R_D C_D)^2}\right)^2 + \omega^2\left(\frac{R_d^2 C_d}{1+(\omega R_d C_d)^2} + \frac{R_D^2 C_D}{1+(\omega R_D C_D)^2}\right)^2\right)}. \tag{8}$$

The total energy stored in the capacitive system at the midpoint of the transition is then estimated as

$$E = \tfrac{1}{2} C_{\mathrm{eq}} V^2. \tag{9}$$

The same expression for the total energy stored in the capacitive system can also be arrived at by estimating the voltage drop across the dielectric layer and droplet capacitances. The voltage drop across the dielectric layer (V_d) and the droplet (V_D) can then be computed using circuit analysis as

$$V_d = \frac{|Z_d|}{|Z_d + Z_D|} V \tag{10}$$

$$V_D = \frac{|Z_D|}{|Z_d + Z_D|} V. \tag{11}$$

The energy stored in the capacitive components of the dielectric layer and the droplet can be expressed as

$$E = \frac{1}{2}\left(C_d V_d^2 + C_D V_D^2\right) = \frac{V^2}{2}\frac{\left(C_d Z_d^2 + C_D V_D^2\right)}{(|Z_d + Z_D|)^2}. \tag{12}$$

The first derivative of this energy distribution yields the actuation force on the droplet at the midpoint of the transition as

$$F = \frac{\mathrm{d}E}{\mathrm{d}x}. \tag{13}$$

Equation (8) represents the frequency-dependent effective system capacitance for the most general case of electromechanical actuation. It is shown below that equation (8) reduces to the various regimes of electromechanical

actuation depending on the properties of the dielectric layer and the droplet, and the ac frequency.

Case (1). Insulating droplet and dielectric layer under ac frequencies (actuation of insulating liquids).

This case is defined by $R_d = \infty$ and $R_D = \infty$. Equation (8) therefore reduces to the following:

$$C_{\text{eq}} = \frac{\left(\frac{1}{C_d} + \frac{1}{C_D}\right)\frac{1}{\omega^2}}{\frac{1}{\omega^4}\left(\frac{1}{R_d C_d^2} + \frac{1}{R_D C_D^2}\right)^2 + \left(\frac{1}{C_d} + \frac{1}{C_D}\right)^2 \frac{1}{\omega^2}}. \tag{14}$$

The first term in the denominator of equation (14) can be shown to be negligible when compared to the second term. Equation (14) therefore reduces to

$$C_{\text{eq}} = \frac{C_d C_D}{C_d + C_D}. \tag{15}$$

The above expression for the equivalent system capacitance corresponds to two capacitors in series. Interestingly, the effective capacitance of the system is independent of the ac frequency. The actuation force will consequently be independent of the frequency of the ac voltage. Equation (15) captures the physics underlying the electrical actuation of perfectly insulating droplets (e.g., transformer oil) on a perfectly insulating dielectric layer (e.g., silicon oxide or Parylene C).

Case (2). Electrically conducting droplet and insulating dielectric layer under ac frequencies (ac electrowetting).

The mathematical conditions for this case are $R_d = \infty$ and $R_D \ll R_d$, for which equation (8) reduces to the following:

$$C_{\text{eq}} = \frac{\frac{1}{\omega^2 C_d} + \frac{R_D^2 C_D}{1+(\omega R_D C_D)^2}}{\left(\frac{R_D}{1+(\omega R_D C_D)^2}\right)^2 + \omega^2\left(\frac{1}{\omega^2 C_d} + \frac{R_D^2 C_D}{1+(\omega R_D C_D)^2}\right)^2}. \tag{16}$$

The above expression can be rearranged as

$$C_{\text{eq}} = \frac{C_d\left(1 + \omega^2 C_d C_D R_D^2 + (\omega R_D C_D)^2\right)(1 + (\omega R_D C_D)^2)}{\left((1 + \omega^2 C_d C_D R_D^2 + (\omega R_D C_D)^2)^2 + \omega^2 C_d^2 R_D^2\right)}. \tag{17}$$

Equation (17) estimates the ac frequency-dependent equivalent system capacitance which is dependent on the dielectric layer and droplet electrical properties. This equation can be used to estimate the actuation force on electrically conducting droplets under ac actuation, i.e., ac electrowetting.

Case (3). Electrically conducting droplet and insulating dielectric layer under dc actuation (classical EW).

DC actuation corresponds to a frequency of zero; equation (17) for ac electrowetting then reduces to

$$C_{\text{eq}} = C_d. \tag{18}$$

The equivalent system capacitance is simply the capacitance of the dielectric layer. A perfectly conducting droplet implies the absence of an electric field inside the droplet; consequently, the entire voltage drop occurs across the dielectric layer. It should be noted that the equivalent capacitance in the present case corresponds to the capacitance of the dielectric layer with an area equal to the droplet area on the actuated electrode. Also, there is no voltage drop across the dielectric layer on the ground electrode on the bottom plate (figure 2), because the droplet is at a uniform potential and grounded. Therefore, the capacitance as obtained from equation (18) represents the exact capacitance (and not an approximation) of the system capacitance.

It should be noted that while equation (18) (for the case of classical EW) represents an exact and accurate capacitance of the system, equations (15) and (17) (for the cases of insulating fluids actuation and ac electrowetting, respectively) represent a simplified analysis (which does not account for electric field fringing) to estimate the system capacitance and the actuation force at the mid-point of transition. More detailed modeling is needed to estimate the actuation force variation along the length of the transition. One example of such a detailed numerical model is that developed by the authors [10] to estimate the actuation force on an insulating droplet as it moves between two parallel plates.

An analysis of equations (15), (17) and (18) shows that the actuation force on a droplet (for a specified geometry and actuation voltage) is maximum for the classical EW regime in which all the voltage drop occurs across the dielectric layer. The actuation force in the case of ac EW is strongly dependent on the ac frequency; the force decreases as the frequency of the applied voltage increases. At sufficiently high ac frequencies the contribution of the droplet electrical conductivity is totally negated and the droplet behaves like an insulating droplet. Thus, from the point of view of the actuation force, it is advantageous to use dc voltages to actuate a droplet (provided that the droplet electrical conductivity is sufficiently high to ensure that all the voltage drop occurs across the dielectric layer).

These concepts can be clearly illustrated by estimating the actuation force at the transition midpoint on three liquid droplets having different electrical conductivities. The three liquids considered have electrical conductivities of 3.56×10^{-4}, 1.47×10^{-3} and 1.47×10^{-2} $S\ m^{-1}$ and correspond to aqueous potassium chloride (KCl) solutions of concentrations 2.2×10^{-5} M, 10^{-4} M and 10^{-3} M, respectively. These liquids are the same as those utilized in the experiments described below in section 3. The ac frequency-dependent actuation force on these droplets is normalized against the classical EW actuation force (i.e., the force on the droplet if the entire actuation voltage drop occurred across the dielectric layer). The ac actuation force at the midpoint of the transition can be obtained using equation (17) as

$$F = \frac{1}{2}V^2\frac{\mathrm{d}C_{\text{eq}}}{\mathrm{d}x} = \frac{1}{2}V^2\frac{\mathrm{d}A}{\mathrm{d}x}\left(\frac{k_d\varepsilon_0}{h}\right) \times \frac{\left(1 + \omega^2\frac{k_d k_D \varepsilon_0^2}{\sigma_D^2}\frac{H}{h} + \left(\omega\frac{k_D\varepsilon_0}{\sigma_d}\right)^2\right)\left(1 + \left(\omega\frac{k_D\varepsilon_0}{\sigma_d}\right)^2\right)}{\left(\left(1 + \omega^2\frac{k_d k_D \varepsilon_0^2}{\sigma_D^2}\frac{H}{h} + \left(\omega\frac{k_D\varepsilon_0}{\sigma_d}\right)^2\right)^2 + \left(\omega\frac{k_d\varepsilon_0}{\sigma_D}\frac{H}{h}\right)^2\right)}, \tag{19}$$

where A is the area of the droplet on the actuated electrode. The normalizing force F_{EW} acting on a droplet under classical EW actuation (utilizing the same voltage V) can be estimated using equations (9), (13) and (18) as

$$F_{EW} = \frac{1}{2}V^2\frac{\mathrm{d}A}{\mathrm{d}x}\left(\frac{k_d\varepsilon_0}{d}\right). \tag{20}$$

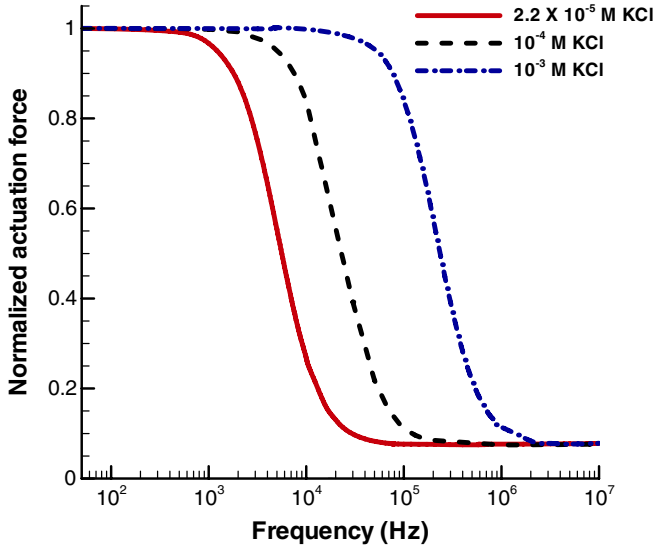

Figure 4. Normalized frequency-dependent actuation force for KCl solutions.

This EW actuation force can be used to normalize the ac actuation force obtained in equation (19) as

$$F_{\text{norm}} = \frac{F}{F_{EW}} = \frac{\left(1+\omega^2\frac{k_d k_D \varepsilon_0^2}{\sigma_D^2}\frac{H}{h}+\left(\omega\frac{k_D\varepsilon_0}{\sigma_d}\right)^2\right)\left(1+\left(\omega\frac{k_D\varepsilon_0}{\sigma_d}\right)^2\right)}{\left(\left(1+\omega^2\frac{k_d k_D \varepsilon_0^2}{\sigma_D^2}\frac{H}{h}+\left(\omega\frac{k_D\varepsilon_0}{\sigma_d}\right)^2\right)^2+\left(\omega\frac{k_d\varepsilon_0}{\sigma_D}\frac{H}{h}\right)^2\right)}. \quad (21)$$

An examination of equation (21) shows that the ac frequency-dependent actuation force (normalized) depends solely on the electrical properties of the dielectric layer and the droplet, the actuation frequency, and the thickness of the droplet and the dielectric, and not on the actuation voltage or droplet size.

Figure 4 is a plot of the normalized actuation force for the three different liquids as a function of the ac frequency as obtained using equation (21). For each liquid, the normalized actuation force is nearly 1 at low ac frequencies; this implies that at low ac frequencies all the voltage drop occurs across the dielectric layer and the actuation force is the same as that for the classical EW (using dc voltages) case. As the frequency increases, the normalized actuation force deviates from the classical EW limit as the electric field penetrates into the droplet. The actuation force then steadily decreases with ac frequency. At sufficiently high ac frequencies the contribution of the droplet electrical conductivity vanishes, and the droplet behaves as electrically insulating; the actuation force does not decrease any further with frequency. This corresponds to the limit of electrical actuation of insulating liquids, and the actuation force can then be predicted using equation (15). An examination of figure 4 also shows that the electrical conductivity of the droplet strongly determines the frequency at which the droplet deviates from the EW limit and the frequency at which it approaches the limit corresponding to actuation of insulating liquids; an increase in the electrical conductivity increases the ac frequencies required to attain these two limits.

In summary, the simplified model in this section has been shown to enable estimation of the actuation force on any droplet in terms of the droplet and dielectric layer electrical properties, the frequency of the applied ac voltage, and the droplet geometry. The model can be used to predict the actuation force across the entire spectrum of electromechanical regimes of actuation; the cases of classical EW actuation and actuation of electrically insulating droplets are the two limits of this spectrum.

3. Experimental measurement of droplet velocities under electrical actuation

3.1. Device fabrication and experimental setup

Detailed experiments were carried out to analyze and understand the predictions from the actuation force model developed in this work. Previous experiments [10] by the authors involved electrical actuation of insulating transformer oil droplets between two flat plates. The present experiments involved electrical actuation of aqueous potassium chloride (KCl) droplets of three different conductivities using ac voltages. The 2.2×10^{-5} M KCl solution was obtained from Hawk Creek Inc., while the 10^{-4} and 10^{-3} M KCl solutions were prepared by mixing the appropriate weight of KCl granules (laboratory grade) in cleanroom-grade deionized water. All devices required for experimentation were fabricated at the Birck Nanotechnology Center at Purdue University. Quartz wafers were used as the bottom plate as shown in figure 1. The actuation electrodes on the bottom plates were microfabricated by patterning a titanium layer, and were interdigitated (as seen in figure 6) to facilitate droplet transport between adjacent electrodes. These electrodes were coated with a Parylene C dielectric layer (0.8 μm) using a vapor deposition process. The Parylene C-covered devices were then coated with a hydrophobic Teflon layer of approximately 500 Å thickness. This was achieved by spinning a 0.1% solution of Teflon-AF 1600 (DuPont, Wilmington, DE) in FC-77 (3M, St. Paul, MN) at 1500 RPM for 30 s and a subsequent hard-baking process on a hot plate at 95 °C for 45 min. The top plate of the device consisted of an indium–tin oxide (ITO)-coated glass slide (Delta Technologies Limited, Stillwater, MN), spin-coated with Teflon. The transparency of the electrically conducting ITO layer permitted imaging of the droplet as it moved between the two plates. Different desired spacings between the top and bottom plates were achieved with the use of 25 μm mica spacers (B & M Co., Inc., Flushing, NY). All the materials used in the fabrication process were of cleanroom grade.

Figure 5 shows a schematic diagram of the experimental setup used for the measurement of droplet velocities. The transition of the droplet from the ground electrode to the actuated electrode was recorded from the top using a high speed camera (Photron Ultima APX, Photron USA Inc., San Diego, CA) attached to a microscope. Images of the droplet transition were recorded at frame rates ranging from 60 to 4000 fps (depending on the measured droplet velocity). The ac voltage required to actuate the droplets was provided by a

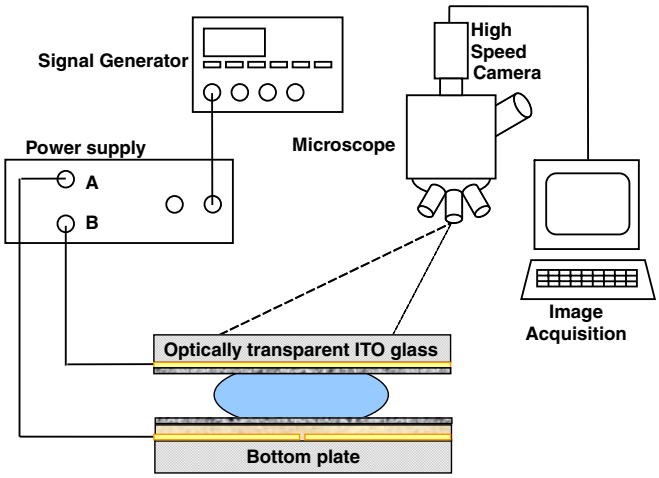

Figure 5. Schematic of the experimental setup used for the measurement of droplet velocities.

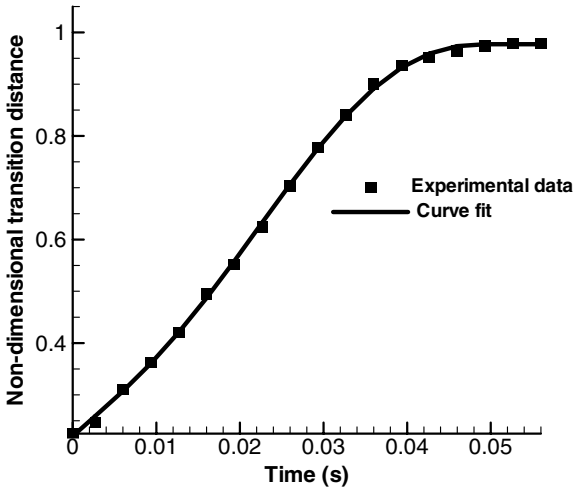

Figure 7. Transition position variation of a 2 mm diameter 10^{-3} M KCl droplet under an ac voltage of magnitude 50 V and frequency 5 kHz.

power supply (Piezo Amplifier EPA-104, Piezo Systems Inc., Cambridge, MA) and a variable frequency signal generator (Tektronix AFG 3022, Tektronix Inc., Richardson, TX). The images were processed using MATLAB [20] to yield the droplet position and velocity. The droplet position was estimated as the average of the leading- and trailing-edge positions at every time instant.

3.2. Droplet velocities under ac electrical actuation

The actuation voltage used in the ac actuation experiments was fixed at an rms value of 50 V and the plate spacing was fixed at 300 μm. The droplet diameter in all the experiments was fixed at $2 \pm 10\%$ mm (in top view). The frequency range utilized in the experiments depended on droplet conductivity and ranged from 50 Hz to 12 kHz for the 2.2×10^{-5} M KCl solution, 50 Hz to 40 kHz for the 10^{-4} M KCl solution and 50 Hz to 500 kHz for the 10^{-3} M KCl solution. At low frequencies (<1 kHz), the droplet shape was observed to change in response to the sinusoidal voltage variation of an ac wave form; at higher frequencies, the droplet inertia prevented it from changing its shape in response to the rapidly changing ac signal. Figures 6(*a*)–(*c*) show a 10^{-3} M KCl droplet during its transition to the actuated electrode at an ac frequency of 50 Hz. Figures 6(*a*)–(*c*) show the starting, intermediate and final positions of the droplet, respectively. It was noted that the droplet continued to flutter about the final position (after the transition) in response to the sinusoidal variation of the ac voltage.

Images of this kind obtained during the droplet transition were processed to obtain the droplet position with time. Figure 7 shows the droplet position (the total transition distance was used to nondimensionalize the transition distance) variation with time for a 2.2×10^{-5} M KCl solution droplet moving under an ac voltage of magnitude 50 V and frequency 5 kHz. A polynomial curve was fit to the results and used to estimate the droplet velocity as a function of the transition position. This methodology was utilized in all the experiments in the present work to estimate droplet velocities.

Figure 8 shows the droplet velocity of a 2.2×10^{-5} M KCl droplet as a function of the transition distance at various ac frequencies (for the same magnitude of the ac voltage). Figure 8 clearly shows that the droplet velocity is strongly influenced by the ac frequency. At each frequency, the droplet velocity is observed to increase to a maximum and then decrease toward the end of the transition. The average and maximum velocities decrease as the ac frequency increases; above 11 kHz, no droplet motion is observed. During the experiments, it was noted that the droplet overshot the actuated

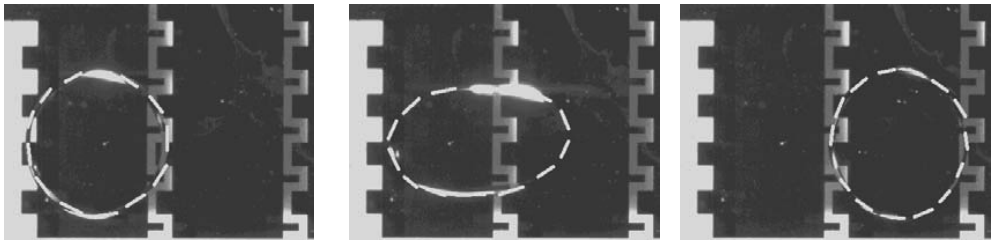

(*a*) t = 0 *s* (*b*) t = 0.006 *s* (*c*) t = 0.03 *s*

Figure 6. Transition of a 2 mm diameter 10^{-3} M KCl droplet under an ac voltage of magnitude 50 V and frequency 50 Hz; the outline of the droplet has been highlighted with a dashed line for easier recognition; (*a*) $t = 0$ s, (*b*) $t = 0.006$ s and (*c*) $t = 0.03$ s.

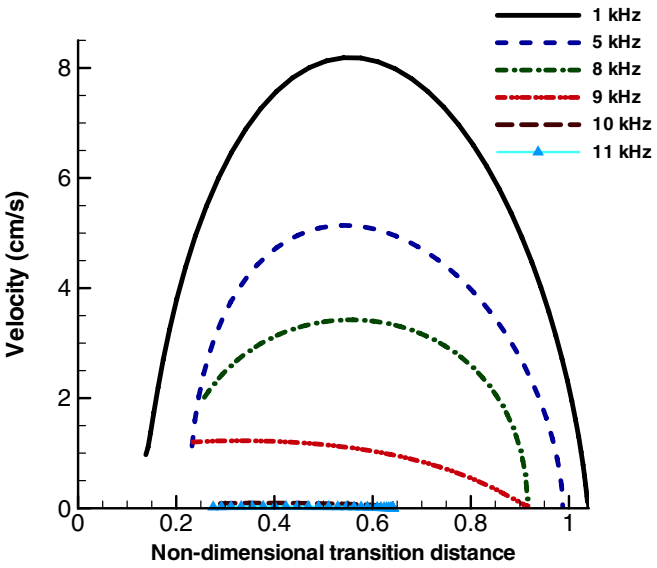

Figure 8. Velocity variation of a 2 mm diameter 2.2×10^{-5} M KCl droplet under an ac voltage of magnitude 50 V at various ac frequencies.

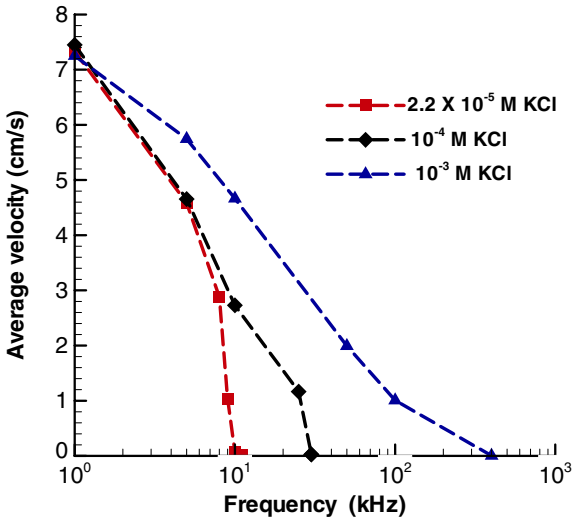

Figure 9. Average velocity of 2 mm diameter KCl solution droplets under an ac voltage of magnitude 50 V versus ac frequency.

electrode at the end of the transition at lower frequencies (such as 1 kHz in the figure) because of sufficiently high velocities during the later stages of the transition. Similar results highlighting the influence of ac frequency on the droplet velocity were also obtained for the 10^{-4} and 10^{-3} M KCl droplets. Additionally, satellite droplets were observed for the 10^{-3} M KCl droplets at frequencies higher than 300 kHz. This phenomenon of satellite droplet emission has been studied in the literature [1, 21]; in the present work, the satellite droplets were neglected in obtaining droplet velocities. No satellite emission was observed for droplets of the 10^{-3} M KCl solution below 300 kHz or for droplets of 2.2×10^{-5} M and 10^{-4} M KCl solutions at any frequency.

Average velocities during transition (for all the three KCl solutions) are shown in figure 9 as a function of the ac

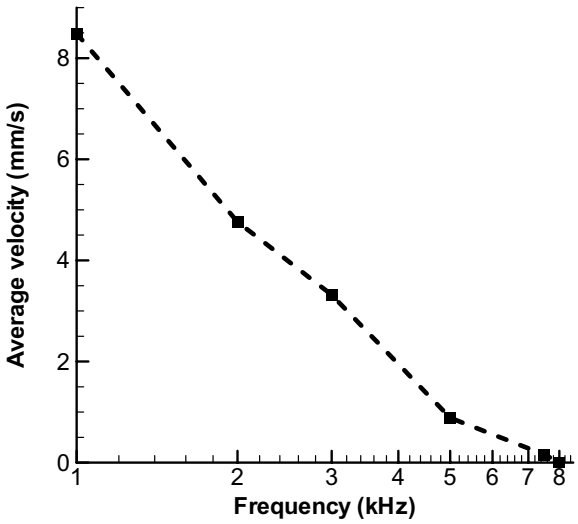

Figure 10. The average velocity of a 2 mm diameter ethylene glycol droplet under an ac voltage of magnitude 50 V versus ac frequency.

frequency. In view of the difficulty in making accurate velocity measurements at the start and end of the droplet transition, all velocity measurements in figure 9 consider droplet motion between 30% and 70% of the total transition distance; the experimental uncertainty in the velocities measured over this distance is estimated to be approximately 10%. It is seen that for all the three liquids, the average velocity decreased as the ac frequency was increased. Above a certain frequency (hereafter called the cut-off frequency for droplet motion), the droplet is observed not to move at all. The cut-off frequency for a given liquid depends on its electrical conductivity and increases as the liquid conductivity increases. For the three liquids considered, the cut-off frequencies were in the range of 11–12, 30–35 and 400–450 kHz for conductivities of 3.56×10^{-4}, 1.47×10^{-3} and 1.47×10^{-2} S m^{-1}, respectively.

The droplet velocity results can be better understood by an examination of the actuation force dependence on the ac frequency and droplet electrical conductivity (figure 4). For a given liquid, increasing the ac frequency reduces the actuation force as shown in figure 4. Above the cut-off frequency for a liquid, the frequency-dependent actuation force is not sufficient to initiate droplet motion by overcoming the contact line friction and other opposing forces; consequently, the droplet fails to move. Combining the results shown in figures 4 and 9, it can be inferred that droplets (of salt solutions of any concentration) stop moving at an ac frequency which results in an actuation force less than approximately 30% of the EW-actuation force.

Another important observation emerges from the comparison of the average velocities under ac actuation with the average velocity under dc actuation (classical EW), utilizing a dc voltage equal to the root-mean-square value of the ac voltage. Experiments were conducted in the same setup to measure the droplet velocities for all the three KCl solutions under dc actuation of 50 V. The experimentally measured average velocities of all the three KCl solution droplets were approximately 4.2 cm s^{-1}, which is less than the average

Table 1. Summary of various electrical actuation schemes.

Regime of actuation	(Droplet/dielectric layer) conductivity	Frequency	Effective capacitance depends on	Typical actuation voltage (V)	Velocity (avg/max) (cm s^{-1})
Actuation of insulating liquids	(0,0)	0 (dc) or finite 0 (dc) or finite (ac)	Droplet and dielectric layer capacitance in series	1000	0.079 / 0.096
Classical (dc voltages) electrowetting	(Finite,0)	0 (dc)	Dielectric layer capacitance only	50	4.2/4.4
AC electrowetting	(Finite,0)	Finite (ac)	Droplet and dielectric layer capacitance, and frequency dependent droplet conductivity	50	7.3/8.2

velocities under low-frequency ac actuation (figure 9, where average velocities of 7.3, 7.4 and 7.3 cm s^{-1} are observed for the three liquid concentrations). This result is non-intuitive because the modeling in the present work shows that the actuation force is maximum for the case of dc actuation. The lower velocities obtained under dc actuation suggest that the forces opposing droplet motion also depend on the nature of electrical actuation (ac versus dc). Berge and Faux [14] demonstrated that the contact-angle hysteresis is lower during ac actuation than with dc actuation; this would reduce the contact-line friction during ac actuation. Reduced contact-line friction can explain the lower velocities under low-frequency ac actuation when compared to dc actuation. Further research is necessary to quantify and understand the mechanism behind the reduction of contact-line friction upon the use of an ac voltage. This reduction in resistance to droplet motion under low-frequency ac voltages increases the attractiveness of using ac voltages instead of dc, besides the advantage that ac voltages reduce the possibilities of chemical reactions within the droplet [5].

All the experiments presented so far involved the use of aqueous KCl solutions. Similar experiments, demonstrating the effect of ac frequency on the droplet actuation force, can also be conducted with any liquid (not necessarily water-based) having a finite electrical conductivity (as demonstrated by Chatterjee *et al* [5]). In the present work, additional experiments were carried out to study the ac voltage-induced electrical actuation of an ethylene glycol (electrical conductivity of 1×10^{-4} S m^{-1} and dielectric constant of 37) droplet between two parallel plates. Figure 10 shows the average velocity of a 2 mm diameter ethylene glycol droplet as a function of the ac frequency for an actuation voltage of 50 V. It is seen that the cut-off frequency for ethylene glycol ranges from 7 to 8 kHz. Also, the magnitudes of the average velocities of ethylene glycol droplets are one order of magnitude less than those of aqueous KCl droplets.

4. Conclusions

The present work analyzed the physics influencing droplet actuation in the electromechanical regimes of classical EW (utilizing dc voltages), EW using ac voltages and the actuation of electrically insulating droplets. It was shown in section 2 that the frequency-dependent effective capacitance of the system is the key determinant of the actuation force acting on the droplet. Table 1 summarizes the key findings from the modeling and experimental results of the present work. The results on the actuation of insulating liquids, as shown in the first row of table 1 are extracted from the previous work of Kumari *et al* [10], which consisted of measuring the velocities of a transformer oil droplet moving between two flat plates using the same experimental setup as described in section 3 of the present work. Table 1 identifies the conditions on droplet and dielectric layer conductivity and the ac frequency which result in either of the three regimes of electromechanical actuation, namely actuation of insulating liquids, classical EW and ac electrowetting. It is seen that significantly lower voltages are required to actuate electrically conducting droplets than insulating ones; further, typical actuation velocities under ac or dc electrowetting are significantly higher than the velocities of insulating liquids. The present work thus sheds light on the physics underlying the various regimes of electromechanical actuation.

References

[1] Mugele F and Baret J C 2005 Electrowetting: from basics to applications *J. Phys.: Condens. Matter* **17** R705–74

[2] Bahadur V and Garimella S V 2006 Energy-based model for electrowetting-induced droplet actuation *J. Micromech. Microeng.* **16** 1494–503

[3] Kim C J 2001 Micropumping by electrowetting *ASME Int. Mechanical Engineering Congress and Exposition (New York)* IMECE2001/HTD-24200

[4] Pollack M G, Shenderov A D and Fair R B 2002 Electrowetting-based actuation of droplets for integrated microfluidics *Lab Chip* **2** 96–101

[5] Chatterjee D, Hetayothin B, Wheeler A R, King D J and Garrell R L 2006 Droplet-based microfluidics with nonaqueous solvents and solutions *Lab Chip* **6** 199–206

[6] Baird E, Young P and Mohseni K 2007 Electrostatic force calculation for an EWOD-actuated droplet *Microfluidics Nanofluidics* **3** 635–44

[7] Oprins H, Vandevelde B, Beyne E, Borghs G and Baelmans M 2004 Selective cooling of microelectronics using electrostatic actuated liquid droplets-modeling and experiments *Int. Workshop on Thermal Investigations of ICs and Systems (Cote d'Azur, France)* pp 207–12

[8] Pellat H 1895 Mesure de la force agissant sur les diélectriques liquides non électrisés placés dans un champ élitrique *C. R. Acad. Sci., Paris* **119** 691–4

[9] Jones T B, Gunji M, Washizu M and Feldman M J 2001 Dielectrophoretic liquid actuation and nanodroplet formation *J. Appl. Phys.* **89** 1441–8

[10] Kumari N, Bahadur V and Garimella S V 2008 Electrical actuation of dielectric droplets *J. Micromech. Microeng.* **18** 085018
[11] Cooney C G, Chen C-Y, Emerling M R, Nadim A and Sterling J D 2006 Electrowetting droplet microfluidics on a single planar surface *Microfluidics Nanofluidics* **2** 435–46
[12] Kumar A, Pluntke M, Cross B, Baret J C and Mugele F 2006 Finite conductivity effects and apparent contact angle saturation in AC electrowetting *Mater. Res. Soc. Symp. Proc.* **899E** 0899-N06–01
[13] Jones T B 2001 Liquid dielectrophoresis on the microscale *J. Electrost.* **51** 290–9
[14] Berge B and Peseux J 2000 Variable focal lens controlled by an external voltage: an application of electrowetting *Eur. Phys. J.* E **3** 159–63
[15] Ko S H, Lee H and Kang K H 2008 Hydrodynamic flows in electrowetting *Langmuir* **24** 1094–101
[16] Hong J S, Ko S H, Kang K H and Kang I S 2008 A numerical investigation on AC electrowetting of a droplet *Microfluidics Nanofluidics* **5** 263–71
[17] Jones T B 2002 On the relationship of dielectrophoresis and electrowetting *Langmuir* **18** 4437–43
[18] Jones T B and Wang K L 2004 Frequency dependent electromechanics of aqueous liquids: electrowetting and dielectrophoresis *Langmuir* **20** 2813–8
[19] Jones T B, Fowler J D, Chang Y S and Kim C J 2003 Frequency based relationship of electrowetting and dielectrophoretic liquid microactuation *Langmuir* **19** 7646–51
[20] MATLABR 2007 2007 *Reference Manual* (Natick, MA: The Mathworks, Inc.)
[21] Vallet M, Vallade M and Berge B 1999 Limiting phenomena for the spreading of water on polymer films by electrowetting *Eur. Phys. J.* B **11** 583–91